PROCEEDINGS, TOUGH Symposium 2006
Lawrence Berkeley National Laboratory, Berkeley, California, May 15–17, 2006

SOME TOPOLOGICAL ASPECTS OF THE (UN) STRUCTURED GENERATION OF MESHES: A POSSIBLE ENHANCEMENT OF MESHMAKER IN TOUGH2

Juan Carlos Díaz Patiño, Ricardo Pacheco Venegas and Mario César Suárez-Arriaga [1]

[1] Faculty of Sciences, Michoacan University - UMSNH
Edificio B, Ciudad Universitaria
Morelia, Michoacán, 58090, México
e-mail: rnoel4@yahoo.com.mx , juancdp@fismat.umich.mx

ABSTRACT

The non-linear partial differential equations solved in TOUGH by the Integral Finite Difference Technique need meshes with diverse degrees of sophistication to model the geometry of physical systems in 2D or 3D domains with boundaries that can be of complex shapes. The main mathematical tools required to create efficient grids are differential geometry, tensor analysis and topology. We present several results from topology and geometry applied to practical grid generation. Structured mesh generation is the first step in the solution of problems with boundary conforming meshes. Structured meshes deal with the construction of coordinate curves in 2D and of coordinate surfaces in 3D. The intersection of these curves and surfaces produces mesh points and cells inside the solution domain. The grid cells are generally four sided geometric objects in 2D and finite volumes with six curved faces in 3D. The connectivity of points is the manner in which grid points are connected to each other in the solution domain. This connectivity depends on the overall generation scheme used. The Cartesian coordinates of every point can be stored in specific matrices with geometric and topological information. A variational approach is used for grid properties (orthogonality, longitude, area and smoothness) that can be controlled by the minimization of a functional. In unstructured meshes the connectivity between grid points can vary from point to point and it has to be described explicitly by an appropriate and particular data structure. This characteristic makes the unstructured solution algorithms more expensive in computational cost but more flexible and useful when employed in adaptive solutions of transient flows and moving boundary problems. This scheme is widely used in many applications of the Finite Element Method and in the Galerkin Discontinuous approach. We introduce an unstructured mesh generation using the Delaunay triangulation in 2D. The Delaunay tetrahedrization holds in 3D. In the first part we work in two dimensions using classic constructions from Euclidean geometry. In the second part we introduce topological concepts to generate meshes in three dimensions. We developed Fortran and Visual C codes to show some results in 2D. The practical aspects of this work could be useful as enhanced options for the TOUGH2 Meshmaker module.

VORONOI DIAGRAMS

Given a finite set of points in the plane, the idea is to assign to each point a region of influence in such a way that the regions decompose the plane. To describe a specific way to do that, let $S \in \mathbb{R}^2$ be a set *of n* points and define the *Voronoi region of* $p \in \mathbb{R}^2$ as the set of points $x \in \mathbb{R}^2$ that are at least as close to p as to any other point in *S;* that is:

$$V_p=\{x \in \mathbb{R}^2 \mid ||x-p|| \leq ||x-q|| \text{ , } "q \in S \} \qquad (1)$$

This definition is illustrated in Figure 1. Consider the half-plane of points at least as close to p as to q: $H_{pq}=\{ x \in \mathbb{R}^2 \mid ||x-p|| \leq ||x-q|| \}$. The Voronoi region of p is the intersection of half-planes H_{pq}, for all $q \in S - p$, it follows that V_p is a convex polygonal region, possibly unbounded, with at most $n - 1$ edges. Each point $x \in \mathbb{R}^2$ has at least one nearest point in S, so it lies in at least one Voronoi region. It follows that the Voronoi regions cover the entire plane. Two Voronoi regions lie on opposite sides of the perpendicular bisector separating the two generating points. It follows that Voronoi regions do not share interior points, and if a point x belongs to two Voronoi regions, then it lies on the bisector of the two generators (Fig. 1). The Voronoi regions together with their shared edges and vertices form the *Voronoi diagram* of S:

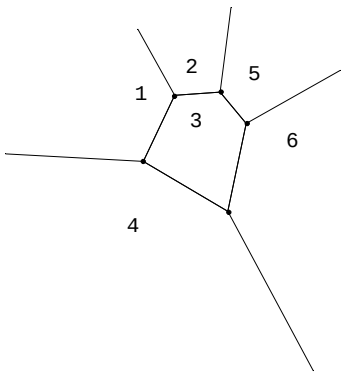

Figure 1. A Voronoi Region in the Plane.

DELAUNAY TRIANGULATION

We get a dual diagram if we draw a straight Delaunay edge connecting the points $p, q \in S$ if and only if their Voronoi regions intersect along a common line segment. In general, the Delaunay edges decompose the convex hull of S into triangular regions, which are referred to as *Delaunay triangles*:

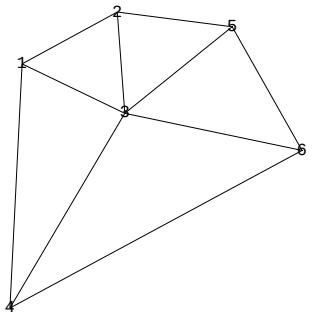

Figure 2. DelaunayTriangles.

To count the Delaunay edges we use some results on *planar graphs,* defined by the property that their edges can be drawn in the plane without crossing. It is true that no two Delaunay edges cross each other, but to avoid an argument, we draw each Delaunay edge from one endpoint straight to the midpoint of the shared Voronoi edge and then straight to the other endpoint (Figs. 2 & 3). It is obvious that any pair of these edges does not cross. With the use of Euler's relation, it can be shown that a planar graph with $n \geq 3$ vertices has at most *3n-6* edges and at most *2n-4* faces. The same bounds hold for the number of Delaunay edges and triangles. There is a bisection between the Voronoi edges and the Delaunay edges, so *3n-6* is also an upper bound on the number of Voronoi edges. Similarly, *2n-4* is an upper bound for the number of Voronoi vertices (Fig. 3).

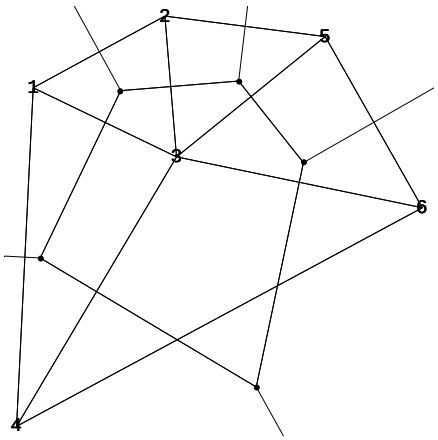

Figure 3. Voronoi and Delaunay edges.

Degeneracy

There is an ambiguity in the definition of a Delaunay triangulation if four or more Voronoi regions meet at a common point *u.* The points generating four or more regions have the same distance from *u:* they lie on a common circle around *u.* Probabilistically, the chance of picking even just four points on a circle is zero because the circle defined by the first three points has zero measure in $\mathbb{R}^2$. A common way to say the same thing is that four points on a common circle form a *degeneracy* or a *special case.* An arbitrarily small perturbation suffices to remove the degeneracy and to reduce the special case to the general case. In this paper we will assume a *general position,* which is the absence of any degeneracy.

Circles and Power

For now we assume *general position*. For a Delaunay triangle, *abc,* consider the circumcircle, which is the unique circle passing through *a, b,* and c. Its center is the corresponding Voronoi vertex, $u = V_a \bigcap V_b \bigcap V_c$, and its radius is $\sigma = \|u - a\| = \|u - b\| = \|u - c\|$. We call the circle *empty* because it encloses no point of *S.* It turns out that empty circles characterize Delaunay triangles.

Circumcircle Claim

Let $S \subseteq \mathbb{R}^2$ be finite and in general position, and let $a, b, c \in S$ be three points. Then *abc* is a Delaunay triangle if and only if the circumcircle of *abc* is empty. It is not entirely straightforward to see that this is true. Instead of proving the Circumcircle Claim, we focus our attention on a new concept of distance from a circle. The *power* of a point $x \in \mathbb{R}^2$ from a circle *U* with center *u* and radius σ is $\pi_U(x) = \|x - u\| - \sigma^2$. If *x* lies outside the circle, then π_U is the square length of a tangent line segment connecting *x* with *U.* In any case, the power is positive outside the circle, zero on the circle, and negative inside the circle. We sometimes think of a circle as a weighted point and of the power as a weighted distance to that point. Given two circles, the set of points with equal power from both is a line.

Acyclicity

We use the notion of power to prove an acyclicity result for Delaunay triangles. Let $x \in \mathbb{R}^2$ be an arbitrary but fixed viewpoint. We say a triangle *abc lies in front of* another triangle *def* if there is a half-line starting at *x* that first passes through *abc* and then

through *def.* We write $abc \prec def$ if *abc* lies in front of *def.* The set of Delaunay triangles together with $\prec$ forms a relation. General relations have cycles, which are sequences $\tau_0 \prec \tau_1 \prec \cdots \prec \tau_k \prec \tau_0$. Such cycles can also occur in general triangulations, but they cannot occur if the triangles are defined by empty circumcircles.

Acyclicity Lemma

The in-front relation for the set of Delaunay triangles defined by a finite set $S \subseteq \mathbb{R}^2$ is acyclic.

Proof: We show that $abc \prec def$ implies that the power of *x* from the circumcircle *of abc* is less than the power from the circumcircle of *def.* Define $abc = \tau_0$ and write $\pi_0(x)$ for the power of *x* from the circumcircle of *abc.* Similarly define $def = \tau_k$ y $\pi_k(x)$. Because *S* is finite, we can choose a half-line that starts at *x,* passes through *abc* and *def,* and contains no point of *S.* It intersects a sequence of Delaunay triangles: $abc = \tau_0 \prec \tau_1 \prec \cdots \prec \tau_k = def$. For any two consecutive triangles, the bisector of the two circumcircles contains the common edge. Because the third point of τ_{i+1} lies outside the circumcircle of τ_i, we have $\pi_i(x) < \pi_{i+1}(x)$. Hence $\pi_0(x) < \pi_k(x)$. The acyclicity of the relation follows because real numbers cannot increase along a cycle.

Edge Flipping

This section introduces a local condition for edges; it implies that a triangulation is of Delaunay type. Here we derive an algorithm based on edge nipping. The correctness of the algorithm implies that, among all triangulations of a given point set, the Delaunay triangulation maximizes the smallest angle.

Empty circles

Recall the Circumcircle Claim, which says that three points $a, b, c \in S$ are vertices of a Delaunay triangle if and only if the circle that passes through *a, b,* c is empty. A Delaunay edge, *ab,* belongs to one or two Delaunay triangles. In either case, there is a pencil of empty circles passing through *a* and *b.* The centers of these circles are the points on the Voronoi edge $V_a \bigcap V_b$. What the Circumcircle Claim is for triangles the Supporting Circle Claim is for edges.

Supporting Circle Claim

R Let $S \subseteq \mathbb{R}^2$ be finite and in general position and let $a, b \in S$. Then *ab* is a Delaunay edge if and only if there is an empty circle that passes through *a* and *b*.

Delaunay lemma

A *triangulation* is a collection of triangles with their edges and vertices. A triangulation *K triangulates S* if the triangles decompose the convex hull of *S* and the set of vertices is *S.* An edge $ab \in K$ *is locally Delaunay* if:

(i) it belongs to only one triangle and therefore bounds the convex hull, or

(ii) it belongs to two triangles, *abc* and *abd,* and *d* lies outside the circumcircle *of abc.*

A locally Delaunay edge is not necessarily an edge of the Delaunay triangulation, and it is fairly easy to construct such an example. However, if *every* edge is locally Delaunay, then we can show that *all* are Delaunay edges circumcircles.

Delaunay Lemma

If every edge of *K is* locally Delaunay, then *K* is the Delaunay triangulation of *S*.

Proof: Consider a triangle $abc \in K$ and a vertex $p \in K$ different from *a, b, c.* We show that *p* lies outside the circumcircle of *abc.* Because this is then true for every *p,* the circumcircle of *abc* is empty and because this is then true for every triangle *abc, K* is the Delaunay triangulation of *S.* Choose a point *x* inside *abc* such that the line segment from *x* to *p* contains no vertex other than *p.* Let $abc = \tau_0, \tau_1, \ldots, \tau_k$ be the sequence of triangles that intersect x*p.* We write $\pi_I(p)$ for the power of *p* to the circumcircle of τ_i, as before. Since the edges along *xp* are all locally Delaunay, we have $\pi_0(p) > \cdots > \pi_k(p)$. Since *p* is one of the vertices of the last triangle, we have $\pi_k(p) = 0$. Therefore $\pi_0(p) > 0$ which is equivalent to *p's* lying outside the circumcircle of *abc*.

Edge-flip algorithm

If *ab* belongs to two triangles, *abc* and *abd,* whose union is a convex quadrangle, then we *flip ab* to *cd.* Formally, this means we remove *ab, abc, abd* from the triangulation and we add *cd, acd, bed* to the triangulation. The picture of a flip looks like a tetrahedron with the front and back superimposed. We can use edge flips as elementary operations to convert an arbitrary triangulation *K* to the Delaunay triangulation. The algorithm uses a stack and maintains the invariant that unless an edge is locally Delaunay, it resides on the stack. To avoid duplicates, we mark edges stored on the stack. Initially, all edges are marked and pushed on the stack.

The general Algorithm

```
While stack is non-empty
 do pop ab from stack and unmark it;
 if ab is not locally Delaunay then
   flip ab to cd;
   for xy ∈ {ac,cb,bd,da} do
      if xy not marked then.
        mark xy and push it on stack
      endif
   endfor
 endif
endwhile.
```

Let *n* be the number of points. The amount of memory used by the algorithm is *0(n)* because there are at most *3n-6* edges, and the stack contains at most one copy of each edge. At the time the algorithm terminates, every edge is locally Delaunay. By the Delaunay Lemma, the triangulation is therefore the Delaunay triangulation of the point set.

Simplicial Complexes

We use simplicial complexes as the fundamental tool to model geometric shapes and spaces. They generalize and formalize the somewhat loose geometric notions of a triangulation. Because of their combinatorial nature, simplicial complexes are perfect data structures for geometric modelling algorithms.

Simplices

A finite collection of points is *affinely independent* if no affine space of dimension *i* contains more than *i +1* of the points, and this is true for every *i.* A *k-simplex* is the convex hull of a collection of *k+1* affinely independent points, $\sigma = conv(S)$*. The dimension of* σ is $\dim \sigma = k$. In $\mathbb{R}^d$, the largest number of affinely independent points is *d+1*, and we have simplices of dimension -1,0,..., *d.* The (-l)-simplex is the empty set. The convex hull of any subset $T \subseteq S$ is again a simplex. It is a subset of *conv(S)* and called a *face* of σ, which is denoted $\tau \le \sigma$. If $\dim \tau = l$ then r is called an *l-face.* $\tau = \varnothing$ and $\tau = \sigma$ are *improper* faces, and all others are *proper* faces of σ. The number of *l* faces of σ is equal to the number of ways we can choose *l + 1* from *k + 1* points, which is equal to $\binom{k+1}{l+1}$. The total number of faces is:

$$\sum_{l=-1}^{k} \binom{k+1}{l+1} = 2^{k+1} \qquad (2)$$

Simplicial Complexes

A *simplicial complex* is the collection of faces of a finite number of simplices, any two of which are either disjoint or meet in a common face. More formally, it is a collection *K* such that:

1) $\sigma \in K \wedge \tau \le \sigma \Rightarrow \tau \in K$ and
2) $\sigma, \upsilon \in K \Rightarrow \sigma \bigcap \tau \le \sigma, \tau.$

Note that $\varnothing$ is a face of every simplex and thus belongs to *K* by Condition 1). Condition 2) therefore allows for the possibility that σ and υ be disjoint.

TOPOLOGY

The most fundamental concept in point set topology is a *topological space,* which is a point set X together with a system *X of* subsets $A \subseteq X$ that satisfies:

1. $\varnothing, X \in \tau$
2. $Z \subseteq \tau$ implies $\bigcup Z \in \tau$, and
3. $Z \subseteq \tau$ and Z finite, implies $\bigcap Z \in \tau$

The system *X* is a *topology* and its sets are the open sets in X. This definition is exceedingly general and non intuitive, but later we will get a better understanding of what is a topological space. The most important example is the *d-dimensional Euclidean space,* denoted as $\mathbb{R}^d$. We use the Euclidean distance function to define an *open ball* as the set of all points closer than some given distance from a given point. The topology of $\mathbb{R}^d$ is the system of open sets, where each open set is a union of open balls. All other topological spaces in this book are subsets of $\mathbb{R}^d$. A *topological subspace* of the pair (X,τ) is a subset $Y \subseteq X$ together with the *subspace topology* consisting of all intersections between Y and open sets, $\tau\big|_Y = \{Y \bigcap A \mid A \in \tau\}$. An example is the *d-ball,* defined as the set of points at distance 1 or less from the origin:

$$B^d = \{x \in \mathbb{R}^d \mid \|x\| \le 1\} \qquad (3)$$

Its open sets are the intersections B^d with open sets in $\mathbb{R}^d$. An open set in B^d is not necessarily open in $\mathbb{R}^d$.

Homeomorphisms

Topological spaces are considered the same or of the same type if they are connected the same way. There are several possibilities to define this notion. The most important one is based on homeomorphisms, which are functions between topological spaces. Such a function is *continuous* if the preimage of every open set is open, and if it is continuous it is referred

to as a *map. A homeomorphism* is a function $f : X \to Y$ that is bijective, continuous, and has a continuous inverse. If a homeomorphism exists then X and Y are *homeomorphic,* and this is denoted as $X \approx Y$. For example, consider the open unit disk which is the set of points in $\mathbb{R}^2$ at distance less than one from the origin. This disk can be stretched over the entire plane. Define $f(x) = x/(1-\|x\|)$, which maps *x* to the point on the same radiating half-line at the original distance times $x/(1-\|x\|)$ from the origin. Function *f* is bijective and continuous, and its inverse is continuous. It follows that the open disk is homeomorphic to R^2. More generally, every open k-dimensional ball is homeomorphic to $\mathbb{R}^k$.

Triangulation

The meaning of the term changes from one area to another. In geometry, there is no generally agreed upon definition, but it usually means a simplicial complex. In topology, a triangulation has a precise meaning, and that meaning is similar to the idea of a mesh that gives combinatorial structure to space. Let *K* be a simplicial complex in $\mathbb{R}^d$. Its *underlying space* is the union of its simplices together with the subspace topology inherited from $\mathbb{R}^2$,

$$|K| = \{ x \in \mathbb{R}^d \mid x \in \sigma \in K \} \qquad (4)$$

A *polyhedron* is the underlying space of a simplicial complex. We can think of *K* as a combinatorial structure imposed on |*K*|. There are others. Using homeomorphisms, we can impose the same structure on spaces that are not polyhedra. A *triangulation* of a topological space X is a simplicial complex *K* whose underlying space is homeomorphic to X, $|K| \approx X$. The space X is *triangulable* if it has a triangulation.

Manifolds

The Manifolds are particularly nice topological spaces. They are defined locally. A *neighborhood* of a point *x* e X is an open set that contains *x.* There are many neighborhoods, and usually it suffices to take one that is sufficiently small. A topological space X is a *k-manifold* if every *x* e X has a neighbourhood homeomorphic to $\mathbb{R}^k$. It is more intuitive to substitute a small open k-ball for $\mathbb{R}^k$, but this makes no difference because the two are homeomorphic. A simple example of a manifold is the *k-sphere,* which is the set of points at unit distance from the origin in the *(k*+1)-dimensional Euclidean space,

$$S^k = \{ x \in \mathbb{R}^{k+1} \mid \|x\| = 1 \}$$

Euler Characteristic

A topological invariant that predated the creation of topology as a field within mathematics is the Euler characteristic of a space. This section introduces the Euler characteristic, talks about shelling, and proves the shellability of triangulations of the disk.

Alternating Sums

The *Euler characteristic* of a simplicial complex *K is* the alternating sum of the number of simplices, where *d = dim K* and *s, is* the number of *i*-simplices in *K.*

$$\chi(K) = s_0 - s_1 + s_2 - \cdots + (-1)^d s_d, \qquad (5)$$

It is common to omit the (-l)-simplex from the sum.

2 - Manifolds

A two-dimensional manifold can be constructed from a piece of paper by gluing edges along its boundary. As an example consider the torus, T, which can be constructed from a square by gluing edges in opposite pairs as shown in Figure 4. The square, together with its two edges and one vertex, forms a cell complex for the torus, with Euler characteristic:

$$\chi(T) = 1 - 2 + 1 = 0 \qquad (6)$$

The straightforward treatment of the torus can be extended to general 2-manifolds by using the complete characterization of 2-manifolds, which was one of the major achievements in nineteenth-century mathematics. The list of orientable 2-manifolds consists of the 2-sphere, the torus with one hole, the torus with two holes, and so on. The number of holes is the *genus* of the 2-manifold. The torus with *g* holes can be constructed from its polygonal schema, which is a regular 4g-gon with edges:

$$a_1 a_2 a_1^{-} a_2^{-} a_3 a_4 a_3^{-} a_4^{-} \cdots a_{2g-1} a_{2g} a_{2g-1}^{-} a_{2g}^{-}, \qquad (7)$$

where an edge without minus sign is directed in anticlockwise and one with minus is directed in clockwise order around the 4g-gon The g-holed torus is constructed by gluing edges in pairs as indicated by the labels. After gluing we are left with *2g* edges and one vertex. The Euler characteristic is therefore $\chi(T_g) = 2 - 2g$. Given a triangulated orientable 2 - manifold, we can use the Euler characteristic to compute the genus and decide the topological type of the 2-manifold.

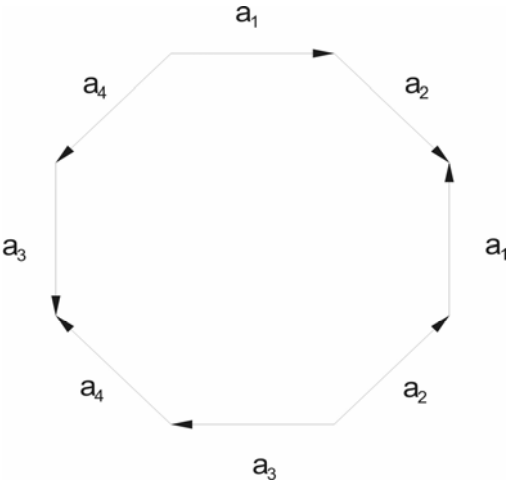

Figure 4. A 2 - Manifold

SOME THEORY AND PRACTICAL ASPECTS OF VARIATIONAL MESH GENERATION

Def. A mesh $X(\varepsilon,\eta) = (x(\varepsilon,\eta), y(\varepsilon,\eta))^t$ over a region $\Omega \subset \mathbb{R}^2$ is a continuous function $X : U_2 \to \Omega$, where U_2 is the unit square $[0,1]\times[0,1]$. The boundaries are: $X(\partial U_2) = \partial\Omega$.

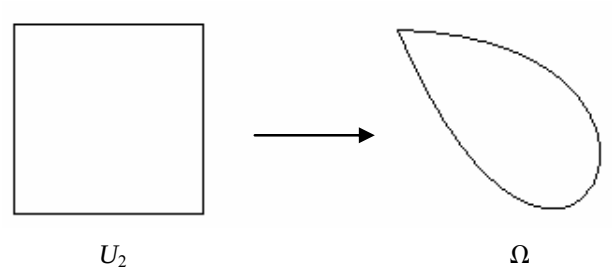

Figure 5. An illustration of the map $X(\varepsilon,\eta)$.

If we consider a coordinate line for ϵ = cte or η = cte inside the unit square, its image will be a curve in Ω. In this way a grid in U_2 will produce a mesh in Ω. Every mesh $X : U_2 \to \Omega$ is associated to a real value by considering some mathematical property: area, longitude, orthogonality and smoothness. This relation will produce a functional of the form:

$$F = \int_0^1\int_0^1 L\left(x_\varepsilon, x_\eta, y_\varepsilon, y_\eta\right) = \int_0^1\int_0^1 L\left(\mathbf{x}_\varepsilon, \mathbf{x}_\eta\right) \qquad (8)$$

This functional can be minimized. Two methods of mesh generation emerge from this minimization. The first method arises by solving the Euler-Lagrange equations; this is called the Continuous Variational Generation. In the second method the functional is discretized first and then a minimization is performed on the multivariate function; this is called the Discrete Variational Generation. In this work we use this latter technique.

DISCRETIZATION OF BARRERA - PEREZ

The functional can be discretized using a bilinear map which allows a better control of the mathematical properties at each cell. Let us assume a rectangular domain Ω and a map *X* defined by:

$$X(\varepsilon,\eta) = A + B\varepsilon + C\eta + D\varepsilon\eta \qquad (9)$$

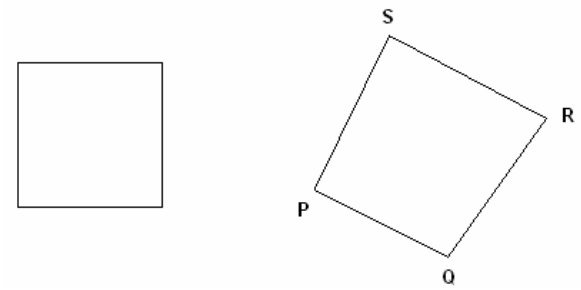

Figure 6. A map X over a rectangle.

The points are: $X(0,0)$ = P, $X(1,0)$ = Q, $X(1,1)$ = R, $X(0,1)$ = S; therefore:

$$X(\varepsilon,\eta) = P + (Q-P)\varepsilon + (S-P)\eta + (R-Q+P-S)\varepsilon\eta \qquad (10)$$

Each functional $\int_0^1\int_0^1 L\left(\mathbf{x}_\varepsilon, \mathbf{x}_\eta\right)$ is replaced by an expression (Tinoco, 1997) of the form: $\sum_{i=1}^{m-1}\sum_{j=1}^{n-1} f_{i,j}$,

Where: $f_{i,j} =$

$$\frac{1}{4}[L\left(X^{ij}{}_\varepsilon(0,0), X^{ij}{}_\eta(0,0)\right) + L\left(X^{ij}{}_\varepsilon(1,0), X^{ij}{}_\eta(1,0)\right) + L\left(X^{ij}{}_\varepsilon(0,1), X^{ij}{}_\eta(0,1)\right) + L\left(X^{ij}{}_\varepsilon(1,1), X^{ij}{}_\eta(1,1)\right)] \qquad (11)$$

And $X^{ij} : U_2 \to \square_{ij}(P,Q,R,S)$ is the map associated to the cell (i, j); but by definition:

$$\begin{aligned} X_\epsilon(0,0) &= X_\epsilon(1,0) = \text{Q} - \text{P}, \\ X_\epsilon(0,1) &= X_\epsilon(1,1) = \text{R} - \text{S}, \\ X_\eta(0,0) &= X_\eta(0,1) = \text{S} - \text{P}, \\ X_\eta(1,0) &= X_\eta(1,1) = \text{R} - \text{Q}. \end{aligned}$$

Therefore:

$$\begin{aligned} f\left(\Delta_{ij}^1\right) &= f\left(\Delta R_{ij}S_{ij}P_{ij}\right) = L\left(X^{ij}{}_\varepsilon(0,1), X^{ij}{}_\eta(0,1)\right) \\ f\left(\Delta_{ij}^2\right) &= f\left(\Delta P_{ij}Q_{ij}R_{ij}\right) = L\left(X^{ij}{}_\varepsilon(1,0), X^{ij}{}_\eta(1,0)\right) \\ f\left(\Delta_{ij}^3\right) &= f\left(\Delta S_{ij}P_{ij}Q_{ij}\right) = L\left(X^{ij}{}_\varepsilon(0,0), X^{ij}{}_\eta(0,0)\right) \\ f\left(\Delta_{ij}^4\right) &= f\left(\Delta Q_{ij}R_{ij}S_{ij}\right) = L\left(X^{ij}{}_\varepsilon(1,1), X^{ij}{}_\eta(1,1)\right) \end{aligned} \qquad (12)$$

With these results we obtain:

$$\sum_{i=1}^{m-1}\sum_{j=1}^{n-1} f_{i,j} = \sum_{i=1}^{m-1}\sum_{j=1}^{n-1}\sum_{k=1}^{4} f\left(\Delta_{ij}^{k}\right) \qquad (13)$$

This expression can be written as:

$$\Delta_{4(m-1)(j-1)+4j-3} = \Delta_{ij}^{1}$$
$$\Delta_{4(m-1)(j-1)+4j-2} = \Delta_{ij}^{2}$$
$$\Delta_{4(m-1)(j-1)+4j-1} = \Delta_{ij}^{3}$$
$$\Delta_{4(m-1)(j-1)+4j} = \Delta_{ij}^{4}$$

We deduce the discrete functional:

$$\sum_{i=1}^{m-1}\sum_{j=1}^{n-1} f_{i,j} = \sum_{i=1}^{4(m-1)(n-1)} f\left(\Delta_i\right) \qquad (14)$$

CLASSIC FUNCTIONALS

Definition: Let ΔPQR be a triangle and:

$$l(\Delta PQR) = \|P-Q\|^2 + \|R-Q\|^2$$
$$\alpha(\Delta PQR) = 2\,Area(\Delta PQR)$$
$$o(\Delta PQR) = (P-Q)^t (R-Q)$$

The classic functionals are:

$$\text{Longitude: } FL = \sum_{i=1}^{4(m-1)(n-1)} l\left(\Delta_i\right) \qquad (15)$$

$$\text{Area: } FA = \sum_{i=1}^{4(m-1)(n-1)} \alpha^2\left(\Delta_i\right). \qquad (16)$$

$$\text{Orthogonality: } FO = \sum_{i=1}^{4(m-1)(n-1)} o^2\left(\Delta_i\right). \qquad (17)$$

$$\text{Smoothness: } FS = \sum_{i=1}^{4(m-1)(n-1)} \frac{l\left(\Delta_i\right)}{\alpha\left(\Delta_i\right)} \qquad (18)$$

APPLICATIONS

In order to illustrate the theory and praxis we have developed and briefly exposed in this work, we present an application of a structured mesh generation for Tejamaniles, the southern sector of the Los Azufres, Mexico geothermal field. Using the available geological and geophysical data, we employ the general two-dimensional contour commonly accepted for this reservoir (Suárez, 1991). Two different meshes were constructed. The first one is a "*coarse*" grid with 1600 curved rectangles. The second one is a global refinement of the first one and contains 10,000 four sided elements. For a reservoir area of approximately 12 Km^2, the local resolution of each mesh is equal to 7500 m^2 /cell and 1200 m^2 /cell respectively. This means an average element size of about 86 x 87 m^2, for the first mesh and of about 34 x 35 m^2, in the refined mesh. Both grids are shown in Figure 7. Nevertheless, it is clear from the numerical results obtained and from this figure that many elements are smaller than the averages, having a real size around 30 x 30 m^2, and 10 x 10 m^2 respectively. Therefore, some portions of the second mesh could be further refined to attain the real local scale of the production and injection wells to simulate their evolution. The construction technique of both meshes is based on the functionals described in the preceding section. A computer code was developed in Visual C language and two graphical results are shown in Figure 7. More results will be presented at the Symposium, including non structured meshes. The code also generates the coordinates of each element of the mesh; it can calculate each element area and the corresponding volume. It is very simple to extend this application to make the code totally compatible with the MESHMAKER module of TOUGH2 (Pruess *et al*., 1999). Potential interested users could obtain a free copy of the code sending a message to the e-mail address at the first page of this paper.

ACKNOWLEDGMENT

The authors wish to express their appreciation for the financial support for this work granted by the Universidad Nacional Autn. de Mexico (UNAM) and by the Universidad Michoacana (UMSNH).

REFERENCES

Pruess, K., C. Oldenburg, and G. Moridis, *TOUGH2 User's Guide, Version 2.0*, Report LBNL-43134, Lawrence Berkeley National Laboratory, Berkeley, Calif., 1999.

Suárez, M. C. *Capacidad Energética del Sector Tejamaniles*. *GEOTERMIA*, Vol. 7, No. 3, pp. 291-324, 1991.

Tinoco, G., *Funcionales Discretos para la Generación de Mallas Suaves y Convexas sobres Regiones Planas Irregulares*, PhD. Thesis, Centro de Investigación en Matemáticas CIMAT, Guanajuato, México, 1997.

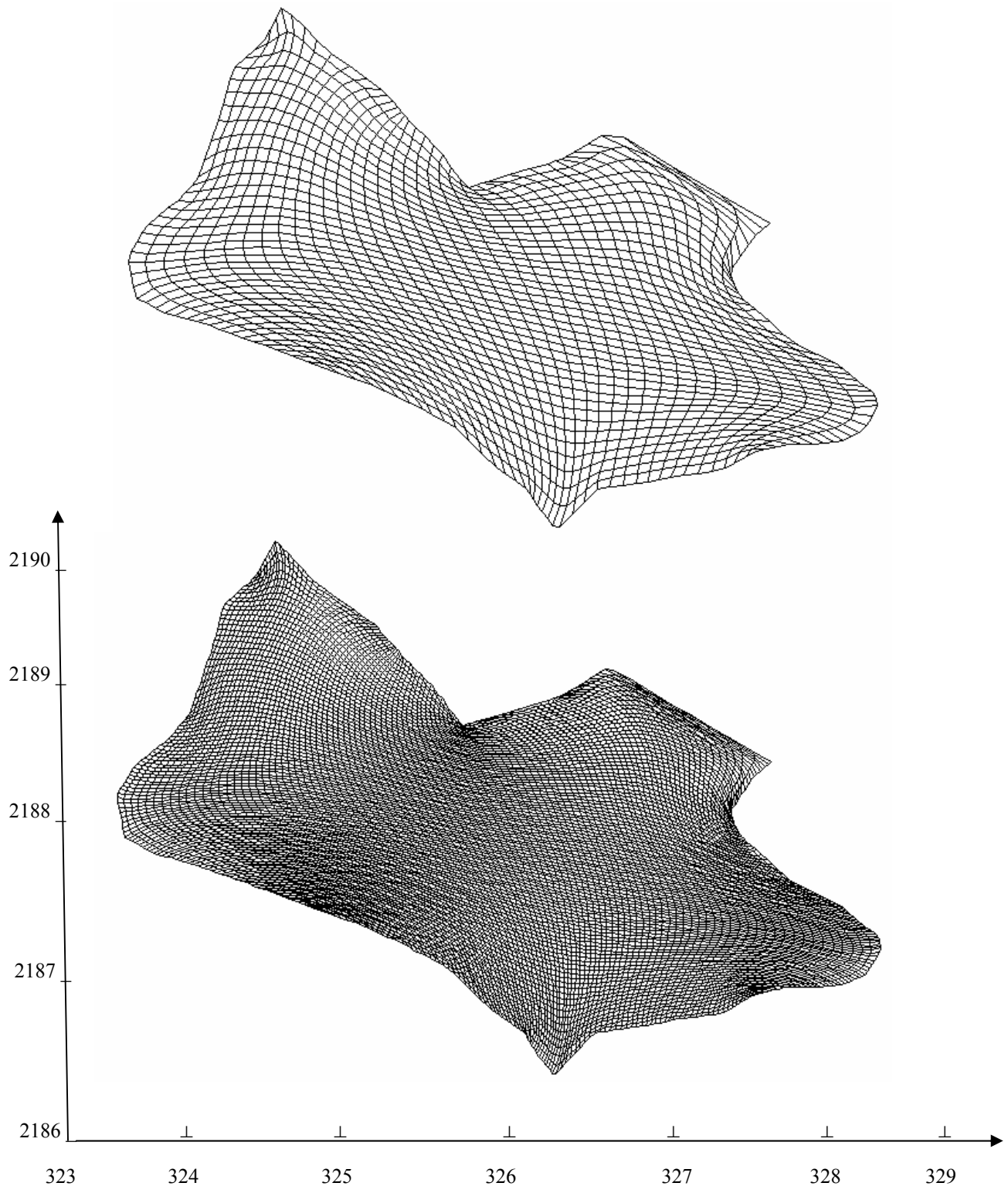

Figure 7. Two structured meshes of the Los Azufres, Mexico geothermal field (southern sector), with 1600 and 10,000 cells respectively. Both meshes are generated using a combination of Area and Longitude Functionals. The axes show approximately the Mercator Coordinates for this reservoir in 10^3 m.

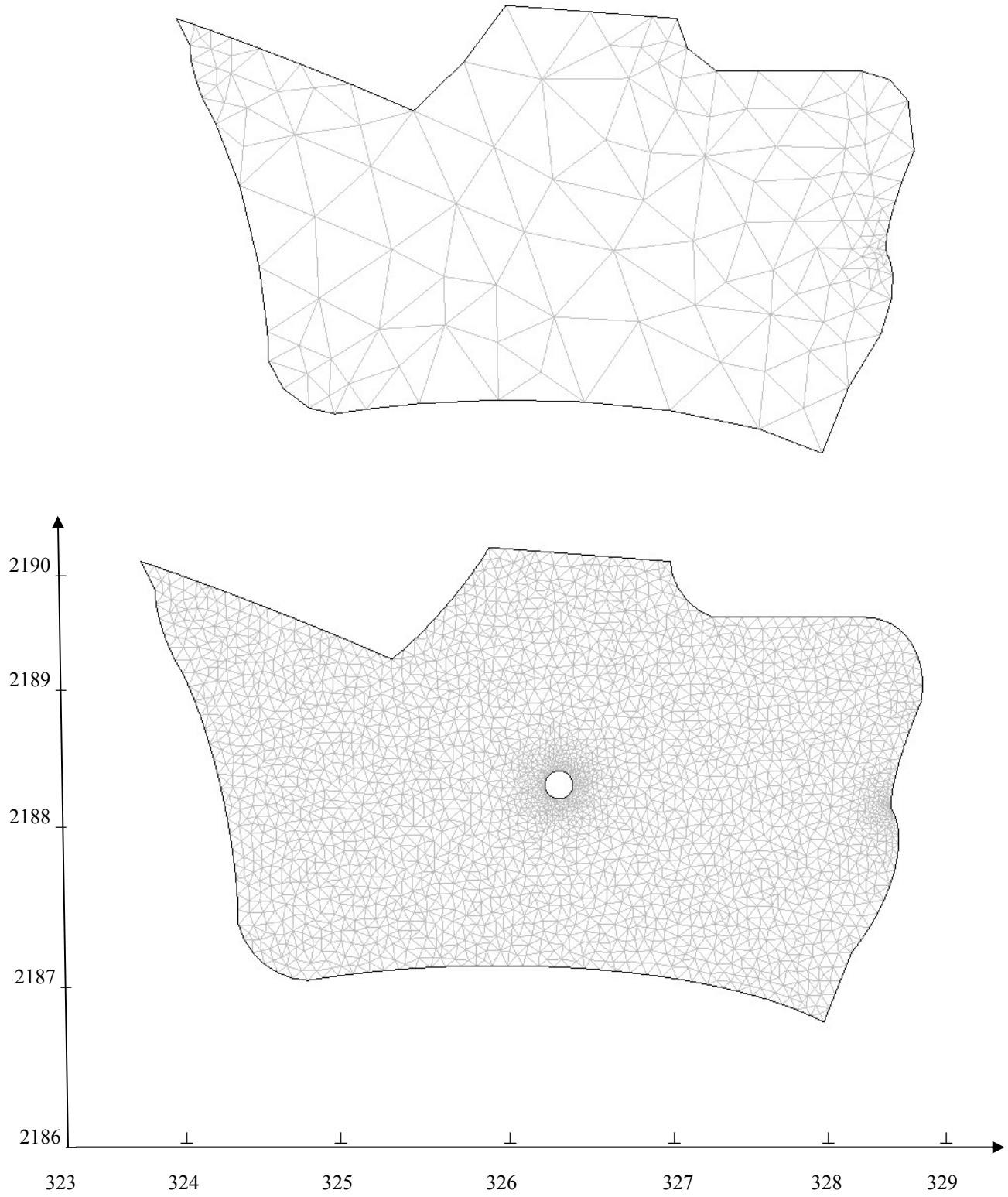

Figure 8. Two unstructured meshes of the Los Azufres, Mexico geothermal field (southern sector), with 256 and 5337 triangles respectively. Both meshes were generated using Delaunay triangulation. The numbers at the axes are approximately the Mercator Coordinates of this reservoir in 10^3 m. The last mesh has a hole to illustrate a forced refinement due to the curvature of the circle.